Fizika Nizkikh Temperatur, 2001, v. 27, Nos. 9/10, p. 1175–1178

Lattice modes of solid nitrogen to 104 GPa

H. Olijnyk and A. P. Jephcoat

Department of Earth Sciences, University of Oxford, Oxford OX1 3PR, UK
E-mail: olijnykHGH@aol.com

Received May 4, 2001

Lattice modes of solid nitrogen were studied by Raman spectroscopy at room temperature to 104 GPa using the diamond anvil technique. Changes in the lattice mode spectral features correlate with those observed in the vibronic spectra suggesting symmetry changes of the crystal lattice. The changes in the spectral features mainly appear as branchings of existing modes supporting the view of a close structural relationship among these high pressure phases.

PACS: **62.50.+p**, **63.20.−e**, **78.30.−j**

1. Introduction

Solid nitrogen exhibits a complicated P–T phase diagram with a variety of different phases, which appears to be well established in the pressure range up to ≈ 20 GPa [1–22]. Above ≈ 20 GPa solid nitrogen is less well understood, both from an experimental and theoretical point of view. Room temperature x-ray diffraction patterns between 16 and ≈ 60 GPa are compatible with the $R\bar{3}c$ structure (ε-phase) [14,16,21]. Raman studies at low temperatures and higher pressures [10,11,18,22–25] suggest several structural modifications above ≈ 25 GPa. Theoretical investigations [26] predicted a tetragonal lattice as stable structure above 20 GPa in disagreement with the experimental results [14,16,21] and calculated pressure-volume relations [27] significantly depart above 12 GPa from accurate equations of state [16]. Since the existence and properties of all these phases are determined by the nature of the intermolecular interactions, these results demonstrate that improvements of the interaction potentials are necessary to correctly describe the properties of solid nitrogen above 20 GPa. In this context, the importance of the anisotropic part of the interaction potential for high-pressure structures of solid nitrogen has been pointed out recently [28,29]. It was shown that the anisotropic term may be important in stabilizing the ε-phase and also influences the orientational behavior of the molecules [28,29]. A stringent test of the intermolecular interaction potentials is provided by lattice modes and their pressure dependencies. In this paper we report Raman measurements of the external modes for pressures up to 104 GPa at room temperature.

2. Experimental

The sample, $^{14}N_2$ enriched with 3% $^{15}N_2$ and 1.4% $^{14}N^{15}N$, was the same for which Raman studies of the internal modes were recently reported [23]. The isotopic mixture was loaded into a high-pressure diamond-anvil-cell at 0.2 GPa using a gas-loading technique [30]. Raman spectra were excited by the 647 nm Kr^+ laser line. Scattered light, collected through a spatial filtering aperture, was analyzed at an angle of 135° with respect to the incoming laser beam using a 0.6-m triple spectrograph and a liquid-nitrogen-cooled CCD multichannel detector. Pressure was determined with the hydrostatic ruby fluorescence scale [31,32]. The peak positions were determined by fitting Voigt profiles to the Raman spectra. This procedure also allows the determination of the frequencies of such modes, which manifest themselves as asymmetries or shoulders in the spectra.

3. Results

Typical Raman spectra of the lattice mode region at various pressures are shown in Fig. 1. One can note that the Raman spectra become increasingly more complex due to the appearance of additional modes as pressure is increased. The mode frequencies and their pressure shifts are shown in Fig. 2. The previous room temperature results of Schneider et al. [18] and Goncharov et al. [25] are also plotted. There is good agreement with the data of Ref. 18 in the common pressure range to 54 GPa, which indicates that any effects on the lattice modes due to the presence of the dilute isotopic species can be neglected in the present study. In the pressure

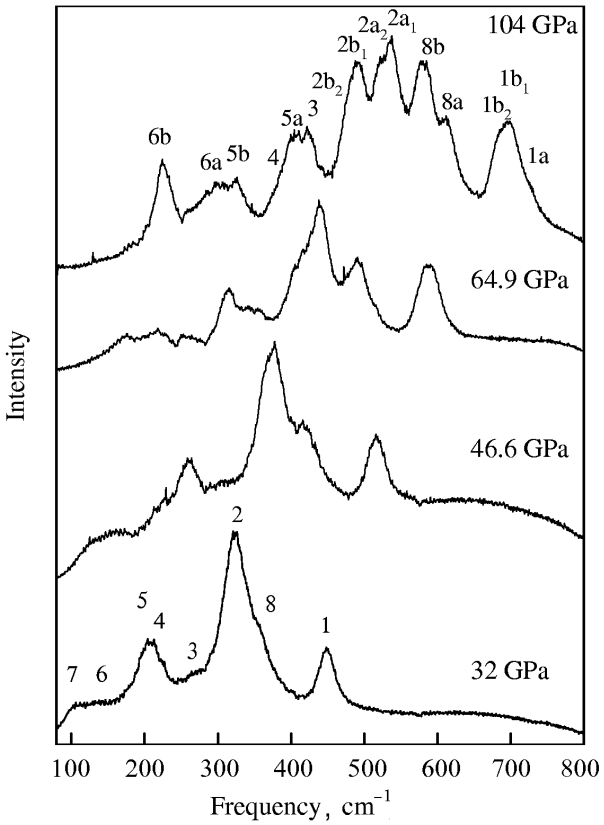

Fig. 1. Lattice mode Raman spectra of solid nitrogen at various pressures.

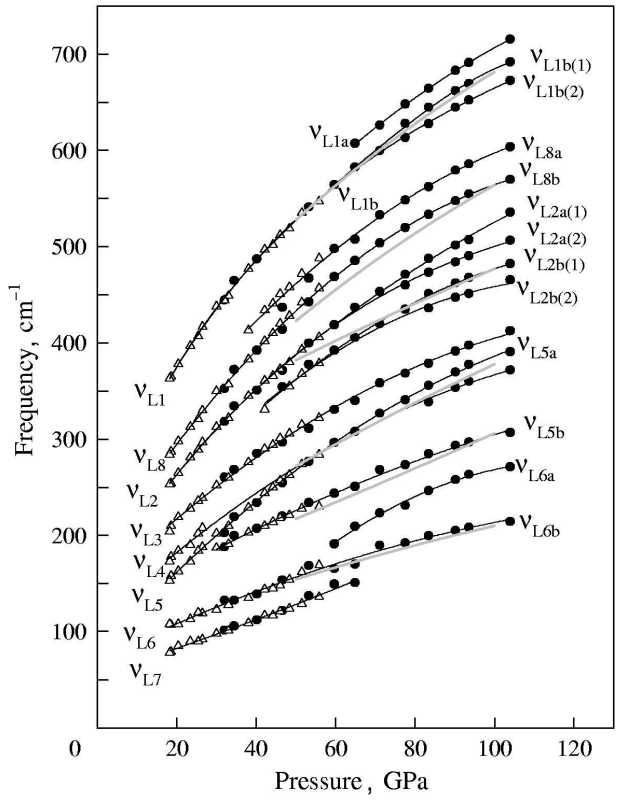

Fig. 2. Pressure shift of lattice mode frequencies of solid nitrogen. Solid circles: present study; open triangles: Ref. 18. Thick grey lines represent the lattice mode data from Ref. 25, which were recorded to ≈ 150 GPa.

range between 50 and 100 GPa Goncharov et al. [25] have reported six external Raman modes whereas in the present study more than these six modes could be resolved in this pressure range as can be noticed in Figs. 1 and 2. All modes show a positive frequency shift, as pressure is increased. In comparison to the earlier high-pressure Raman studies the following additional observations have been made in the present investigation. New modes, ν_{L6a} and ν_{L1a}, appeared around 60 GPa and further splittings, $\nu_{L2a} \rightarrow \nu_{L2a(1)}$, $\nu_{L2a(2)}$ and $\nu_{L1b} \rightarrow \nu_{L1b(1)}$, $\nu_{L1b(2)}$ can be observed around 80 GPa. With the exception of ν_{L7}, which becomes difficult to observe above 60 GPa, all modes already present in the ε-phase above 16 GPa are still existent at the maximum pressure. Above 80 GPa mode ν_{L4}, which merges into mode ν_{L5a} around 25 GPa, reappeared a few wavenumbers below mode ν_{L5a}, indicating crossing of modes ν_{L5a} and ν_{L4} around 55 GPa. The frequency–pressure data are well represented by the expression

$$\nu(P)/\nu_0 = [1 - (\delta_0'/\delta_0)P]^{-\delta_0^2/\delta_0'} \qquad (1)$$

with ν_0 is the mode frequency at $P = 0$ GPa, $\delta_0 = (d \ln \nu/dP)_{P=0}$ the logarithmic pressure coefficient and δ_0' the pressure derivative of δ for $P = 0$. The pressure coefficients for the lattice modes are collected in Table 1.

Table 1

Pressure coefficients and mode Grüneisen parameters of lattice modes of solid nitrogen for the pressure range from 16 to 104 GPa

Mode	ν_0, cm^{-1}	δ_0, GPa^{-1}	δ_0', GPa^{-2}	γ
ν_{L1a}	249.9	0.05457	−0.00781	–
$\nu_{L1b(1)}$	141.2	0.2201	−0.124	1.51
$\nu_{L1b(2)}$	130.5	0.3191	−0.2780	1.51
ν_{L8a}	157.3	0.109	−0.02956	1.59
ν_{L8}, ν_{L8b}	90.87	0.3242	−0.2481	1.71
$\nu_{L2a(1)}$	97.40	0.1777	−0.06896	1.72
$\nu_{L2a(2)}$	79.98	0.3564	−0.3062	1.72
$\nu_{L2b(1)}$	126.0	0.09057	−0.01887	1.83
$\nu_{L2b(2)}$	119.2	0.1479	−0.0599	1.83
ν_{L3}	91.25	0.1409	−0.04678	1.59
ν_{L4}	69.23	0.1606	−0.05489	1.79
ν_{L5}, ν_{L5a}	37.87	0.3404	−0.2039	2.23
ν_{L5b}	98.62	0.04155	−0.00338	1.54
ν_{L6a}	46.20	0.08627	−0.01102	–
ν_{L6}, ν_{L6b}	59.10	0.05706	−0.00626	1.62
ν_{L7}	55.52	0.02308	−0.0003884	2.04

We have determined the mode Grüneisen parameters $\gamma_i = -d \ln \nu_i / d \ln V$ for the lattice modes. The $V(P)$ values were obtained from the $P-V$ data of Refs. 14 and 16 using a Birch–Murnaghan equation of state with bulk modulus $B_0 = 2.55$ GPa, its pressure derivative $B_0' = 3.97$ and $V_0 = 50.99$ Å^3/molecule. The average values of the γ_i's thus obtained for the pressure range 16–65 GPa are also given in Table 1.

4. Discussion

The available x-ray diffraction data [14,16,21] are compatible with the $R\bar{3}c$ lattice above 16.3 GPa and indicate a phase transition around 60 GPa by clear changes in the x-ray diffraction pattern [14]. The $R\bar{3}c$ lattice of the ε-phase is a slight distortion of the cubic δ-phase and has two inequivalent sites, which correspond to the disk-like and sphere-like site of the δ-phase, respectively [12]. In the lattice-mode region eight Raman-active modes are allowed for $R\bar{3}c$, two of which are librons and originate from the former sphere-like site, whereas the remaining six modes are of translational character and are associated with the disk-like site [10].

The observed branchings or appearance of new lattice modes around 30, 40, 65 and 80 GPa correlate well with the branchings observed for the internal modes of the host [11,18,23] as well as of the dilute isotopic species [23], as can be noted from the summary of Table 2.

Table 2

Summary of branchings of lattice and vibronic modes in solid N_2. The number of inequivalent sites is determined from the splittings of the isotopic guest vibrons [23]

Branching pressure	Lattice modes: [18], present study	Host vibrons [23]	Dilute guest vibrons [23]	Number of inequivalent sites
≈ 30 GPa	ν_{L5b}	ν_{2a}	ν_{2a}, ν_{2b}	3
≈ 40 GPa	ν_{L2b}, ν_{L8a}	$\nu_{2c(2c)}$	ν_{2c2}	≥ 4
≈ 65 GPa	ν_{L6a}, ν_{L1a}	$\nu_{2c(2b)}$	ν_{2c1}	≥ 5
≈ 80 GPa	$\nu_{L1b(1,2)}$, $\nu_{L2a(1,2)}$, $\nu_{L2b(1,2)}$	$\nu_{2c(1a)}$	splitting of ν_{2c2}	≥ 6

The branchings in the internal modes occur only in the ν_2 branch, which is related to the molecules on the disk-like site. The splittings, observed in the dilute isotopic species, are thought to result from nonequivalent sites, since factor-group interactions, an alternative explanation for the splitting, are switched off at these small concentrations [23].

Above 30 GPa, with nine lattice modes present, Raman spectra of the external modes are no longer compatible with $R\bar{3}c$, as are the vibronic spectra, which contrasts with the lack of change observed in the x-ray diffraction patterns in this pressure range. These changes in the spectral features might be due to slight modifications in the lattice symmetry, possibly due to subtle changes in the orientation of molecules at the disk-like site, which may lead to two sites with slightly different symmetry. Similar arguments may also be valid for the 40 GPa branching. Another possibility might be that these branchings indicate the onset of the phase transition, which has been observed by clear changes in the x-ray diffraction pattern [14] around 60 GPa and which would then occur gradually over a large pressure range. In this connection it is interesting to note, that the boundary between the ε-phase and the higher-pressure ζ-phase [24], extrapolated to room temperature, implies an $\varepsilon \rightarrow \zeta$ transition at 50–60 GPa. The 80 GPa branching has also been interpreted as an indication of a further phase transition, which is supported by the observed splitting of the ν_{2c2} mode of the $^{15}N_2$ isotopic species. One characteristic feature common to both the external and internal modes is the persistence of the lower pressure modes at the highest pressures, which implies a close structural relationship among the various high-pressure phases.

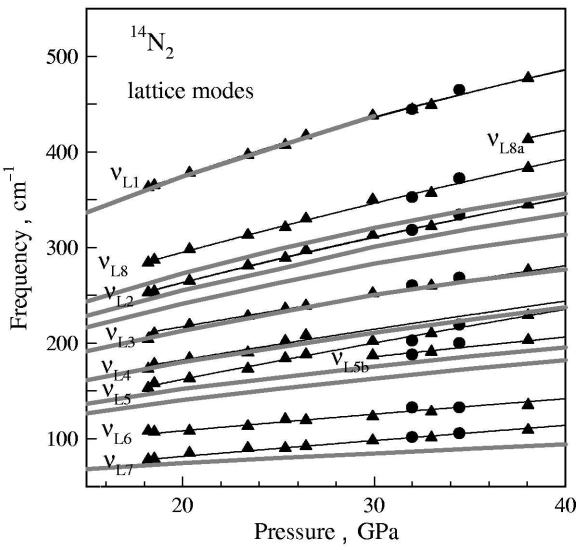

Fig. 3. Thick grey solid lines are the calculated Raman-active lattice-mode frequencies for the $R\bar{3}c$ phase from Ref. 27. Solid triangles (Ref. 18) and solid circles (present study) are the experimentally-observed frequencies.

The observed lattice mode frequencies are compared with calculated frequencies of the $R\bar{3}c$ lattice [27] to 40 GPa in Fig. 3. The calculated frequencies of modes ν_{L1}, ν_{L3} and ν_{L4} are in very good agreement with experiment, whereas for the other modes the good agreement found at lower pressures [27] gets lost at higher pressures. Possible reasons for this increasing discrepancy might involve the inadequacy of the interaction potential, used in these calculations, at higher pressures, a different crystal structure above 30 GPa as well as finite temperature effects.

5. Conclusion

Raman spectra of the lattice modes of solid N_2 are compatible with the $R\bar{3}c$ structure between 16.3 GPa and ≈ 30 GPa. At higher pressures (30, 40, 65 and 80 GPa) changes in the spectral features of the lattice modes correlate with changes in the spectral features of the internal modes probably related to changes in the lattice symmetry. The persistance of the low-pressure modes to the highest pressures, also observed for the internal modes, supports the argument of a close structural relationship among these high-pressure phases. The present data on lattice modes provide additional constraints, which have to be considered in future theoretical attempts of a quantitative interpretation of highly compressed solid nitrogen.

1. W. E. Streib, T. H. Jordan, and W. N. Lipscomb, *J. Chem. Phys.* **37**, 2962 (1962).
2. R. L. Mills and A. F. Schuch, *Phys. Rev. Lett.* **23**, 1154 (1969).
3. F. Schuch and R. L. Mills, *J. Chem. Phys.* **52**, 6000 (1970).
4. J. A. Venables and C. A. English, *Acta Crystallogr.* **B30**, 929 (1974).
5. R. LeSar, S. A. Ekberg, L. H. Jones, R. L. Mills, L. A. Schwalbe, and D. Schiferl, *Solid State Commun.* **32**, 131 (1979).
6. D. T. Cromer, R. L. Mills, D. Schiferl, and L. A. Schwalbe, *Acta Crystallogr.* **B37**, 8 (1981).
7. D. Schiferl, D. T. Cromer, R. R. Ryan, A. C. Larson, R. LeSar, and R. L. Mills, *Acta Crystallogr.* **C39**, 1151 (1983).
8. B. M. Powell, G. Dolling, and H. F. Nieman, *J. Chem. Phys.* **79**, 982 (1983).
9. S. Buchsbaum, R. L. Mills, and D. Schiferl, *J. Phys. Chem.* **88**, 2522 (1984).
10. D. Schiferl, S. Buchsbaum, and R. L. Mills, *J. Phys. Chem.* **89**, 2324 (1985).
11. R. Reichlin, D. Schiferl, S. Martin, C. Vanderborgh, and R. L. Mills, *Phys. Rev. Lett.* **55**, 1464 (1985).
12. R. L. Mills, B. Olinger, and D. T. Cromer, *J. Chem. Phys.* **84**, 2837 (1986).
13. S. Zinn, D. Schiferl, and M. F. Nicol, *J. Chem. Phys.* **87**, 1267 (1987).
14. A. P. Jephcoat, R. J. Hemley, H.-K. Mao, and D. E. Cox, *Bull. Am. Phys. Soc.* **33**, 522 (1988).
15. D. Schiferl, R. LeSar, and D. S. Moore, in: *Simple Molecular Systems at Very High Density*, A. Polian, P. Loubeyre, and N. Boccara (eds.), Plenum Press, New York (1989), p. 303 and references therein.
16. H. Olijnyk, *J. Chem. Phys.* **93**, 8968 (1990).
17. B. J. Baer and M. Nicol, *High Pressure Res.* **4**, 511 (1990).
18. H. Schneider, W. Haefner, A. Wokaun, and H. Olijnyk, *J. Chem. Phys.* **96**, 8046 (1992).
19. M. I. M. Scheerboom and J. A. Schouten, *Phys. Rev. Lett.* **71**, 2252 (1993).
20. M. I. M. Scheerboom and J. A. Schouten, *J. Chem. Phys.* **105**, 2553 (1996).
21. M. Hanfland, M. Lorenzen, C. Wassilew-Reul, and F. Zontone, in: *Abstracts of the International Conference on High Pressure Science and Technology*, Kyoto, Japan, 1997, p. 130.
22. R. Bini, M. Jordan, L. Ulivi, and H. J. Jodl, *J. Chem. Phys.* **108**, 6869 (1998).
23. H. Olijnyk and A. P. Jephcoat, *Phys. Rev. Lett.* **83**, 332 (1999).
24. R. Bini, L. Ulivi, J. Kreutz, and H. J. Jodl, *J. Chem. Phys.* **112**, 8522 (2000).
25. A. F. Goncharov, E. Gregoryanz, H.-K. Mao, Z. Liu, and R. J. Hemley, *Phys. Rev. Lett.* **85**, 1262 (2000).
26. J. Belak, R. LeSar, and R. D. Etters, *J. Chem. Phys.* **92**, 5430 (1990).
27. R. D. Etters, V. Chandrasekharan, E. Uzan, and K. Kobashi, *Phys. Rev.* **B33**, 8615 (1986).
28. A. Mulder, J. P. J. Michels, and J. A. Schouten, *J. Chem. Phys.* **105**, 3235 (1996).
29. A. Mulder, J. P. J. Michels, and J. A. Schouten, *Phys. Rev.* **B57**, 7571 (1998).
30. A. P. Jephcoat, H.-K. Mao, and P. M. Bell, in: *Hydrothermal Experimental Techniques*, G. C. Ulmer and H. L. Barnes (eds.), Wiley Interscience, New York (1987), p. 469.
31. R. A. Forman, G. J. Piermarini, J. D. Barnett, and S. Block, *Science* **176**, 284 (1972).
32. H.-K. Mao, J. Xu, and P. M. Bell, *J. Geophys. Res.* **91**, 4673 (1986).